iJRASET
International Journal For Research in Applied Science and Engineering Technology

INTERNATIONAL JOURNAL FOR RESEARCH

IN APPLIED SCIENCE & ENGINEERING TECHNOLOGY

Volume: 3 **Issue:** I **Month of publication:** January 2015

DOI:

www.ijraset.com

Call: 08813907089 | E-mail ID: ijraset@gmail.com

ISSN: 2321-9653
International Journal for Research in Applied Science & Engineering Technology (IJRASET)

An Advanced Current Controller Implemented with ANN Technique for Three Phase Shunt Active Power Filter

A. Sundararao[1], CH. Sujatha[2]
M.Tech scholar, Assoc. Professor, Department of EEE, Gudlavalleru Engineering College, Gudlavalleru, A.P, India

Abstract— This paper proposes an advanced control strategy to enhance performance of shunt active power filter (APF). The proposed control scheme requires only two current sensors at the supply side and does not need a harmonic detector. In order to make the supply currents sinusoidal, an effective harmonic compensation method is developed with the ANN technique. The absence of the harmonic detector not only simplifies the control scheme but also significantly improves the accuracy of the APF, since the control performance is no longer affected by the performance of the harmonic process. Furthermore tracking, the total cost to implement the proposed APF becomes lower, owing to the minimized current sensors and the use of a four-switch three-phase inverter..

Index Terms—Active power filters (APFs), harmonic current compensation, power quality, resonant controller, ANN.

I. INTRODUCTION

The increasing use of nonlinear loads such as adjustable speed drives, electric arc welders, and switching power supplies causes large amounts of harmonic currents inject into distribution systems. These harmonic currents are responsible for voltage distortion, increasing power losses and heat on networks and transformers, and causing operational failure of electronic equipment. Due to these problems, harmonic restriction standards such as IEEE-519 or IEC 61000-3-2 have been published to demand those harmonic currents injected into utility networks to be below the specified values [1], [2]. In order to improve the power quality of distribution networks as well as to meet these restriction standards, two main solutions have been introduced: *LC* passive filters and Active power filters (APFs) [3]–[5]. *LC* passive filters are traditionally utilized to compensate the harmonic currents since they are simple and low-cost solution. However, they are often large and heavy. Furthermore, the compensation capability of a passive filter is typically fixed and relies heavily on a network's impedance, thus potentially causing undesired resonance problems [5].

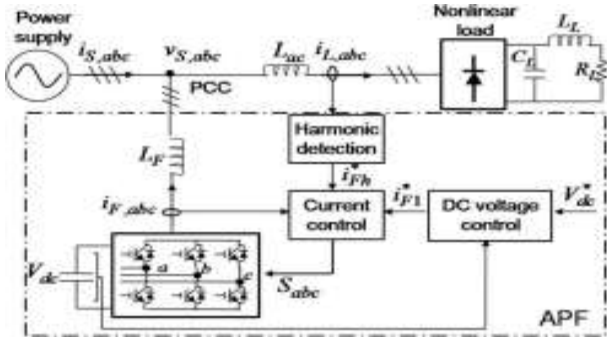

Fig.1.Typical control scheme of a shunt APF.

In contrast, shunt APFs are recognized as a flexible solution for harmonic current compensation since they are capable of compensating harmonic currents generated by many types of nonlinear loads as well as providing fast responses to load variations [3]–[5]. A typical control scheme of a shunt APF is illustrated in Fig. 1. The purpose of an APF is to generate harmonic currents ($i_{F,abc}$) having the same magnitude and opposite phase with the harmonics produced by the nonlinear load, and to ensure that the supply currents ($i_{S,abc}$) contain only the fundamental component. In order to realize the desired goals, as shown in Fig. 1, the

traditional control scheme requires several steps such as load current measurement, harmonic current detection, reference filter current generation, and filter current control [6]–[13], [15]–[18]. Since the APF must generate non-sinusoidal currents, the design of the current controller for the APF is a challenging task. Various control methods have been developed in the literature such as proportional-integral (PI) control [6], [8]–[10], dead-beat control [7], and hysteresis control [6],PI+VPI controller. Due to the limitation of the control bandwidth, the PI controller is not a suitable solution for the APF applications since the current controller must deal with harmonic currents, which are high-frequency signals. In contrast, the dead-beat control method is able to provide fast control response, but the control performance relies significantly on knowledge of the APF parameters. Despite the simple and robust feature of the hysteresis controller, this approach also has an inherent drawback: switching frequency variation, which causes a difficulty in design of an output filter for the APF and results in unwanted resonance problems with the networks. In addition, in order to achieve good current performance, the hysteresis band must be set as small as possible. It results in a significant increasing of the switching frequency and consequently introduces higher switching loss on the APF. In recent years, several high-performance current controllers have been developed for APFs to achieve good control performance [15]–[18]. In these control schemes, the current controllers are employed in the fundamental reference frame, consisting of a proportional controller plus multiple sinusoidal signal integrators [15], a PI controller plus a series of resonant controllers [16], [17], or vector PI (VPI) controllers [18]. In fact, the VPI controller introduced in [18] is an alternative version of resonant controller that has superior and robust characteristics when compensating high-order harmonic currents, but complexity is increased to eliminate h0monics. These control schemes are capable of providing good control performances thanks to high-performance current controllers. However, as illustrated in Fig. 1, the performance of the APF relies on not only the current controller but also the harmonic currents detector. The harmonic detector aims to extract the harmonic components presented in the load currents whose output becomes the reference filter current for the APF. Thus, the performance of this process critically impacts on the accuracy of the APF. The harmonic detector is typically employed by using filters such as high-pass, low-pass, adaptive filters [8]–[13], or through complex mathematical functions [14]. However, by using these filters, it is difficult to achieve both fast response and good steady-state harmonic tracking performance because of a compromise: if the filters are designed to achieve good steady-state performance, their response becomes slow and vice-versa. As a result, the use of a harmonic detector in the control scheme may have an adverse effect on both the accuracy and response of an APF. In order to avoid the use of harmonic detectors, indirect cur-rent control schemes have been introduced in [19]–[24] where the supply currents ($i_{S,abc}$) are directly measured and regulated to be sinusoidal. In [19], [20], [22], hysteresis controller was used in the current control loop to force the supply current to be sinusoidal. However, as mentioned earlier, this method has a drawback, i.e., the variation of the switching frequency, so that the supply current regularly contains many switching noises. Meanwhile, the PI controller and the proportional controller are utilized in [21] and [23], respectively. They obviously have a limitation on the control bandwidth and are unable to accurately regulate high-frequency signals such as harmonic currents. Consequently, it is hard to achieve a good performance of the supply currents. In [24], authors demonstrated that indirect control method is able to provide better performances compared to direct one since it can prevent inaccurate tracking performances of the harmonic detector. Nevertheless, in this control scheme, two sets of current sensors are required. In addition, the reference supply current is given based on the supply voltage which is assumed to be a pure sinusoidal waveform. Thus, the performance of the supply current is degraded when the supply voltage is distorted. Adopting the advantage of indirect current control schemes, i.e., the absence of a harmonic detector, this paper proposes an advanced control strategy to enhance the APF performance. In the proposed control scheme, the supply currents are directly measured and regulated to be sinusoidal by an effective harmonic compensator, which is developed based on a ANN technique and implemented in the fundamental reference frame. Owing to the effectiveness of the proposed ANN controller, the harmonic currents produced by the nonlinear load can be accurately compensated without the demand of a load current measurement and harmonic detector. The absence of the harmonic detector not only simplifies the control scheme but also significantly improves the accuracy of the APF since the control performance is no longer affected by the performance of the harmonic tracking process. Moreover, the total cost to implement the proposed APF is lower, owing to the minimized current sensors and the use of a four switch three-phase inverter (FSTPI). Despite the simplified hardware, the performance of the APF is significantly improved compared to the traditional control scheme thanks to the superiority of the proposed compensation scheme. And also, the proposed control algorithm is capable of mitigating harmonic currents as well as reactive power to achieve unity power factor condition at the supply side.

II. PROPOSED CONTROL STRATEGY TO IMPROVE APF PERFORMANCE

A. Structure of a Shunt APF

Three-phase diode rectifiers are widely used as the front-ends of industrial ac drives [3]–[5]. These types of loads introduce harmonic currents into the networks, which have odd orders: $6n \pm 1 (n = 1, 2, 3 \ldots)$ of the fundamental frequency. Since these harmonic currents cause serious problems and deteriorate the power quality of the distribution networks, the shunt APF was developed to compensate those harmonic currents and consequently to improve the power quality. As illustrated in Fig. 1, a shunt APF is basically a three-phase voltage source inverter (VSI) connected in parallel with a nonlinear load at the point of common coupling through an inductor L_F . The energy storage of the APF is a large capacitor located at the dc-link side of the inverter. The nonlinear load can be presented as a RL or RLC load connected to the power supply through a three-phase diode rectifier as shown in Fig. 1. As stated earlier, the APF must generate the harmonic currents to compensate harmonics produced by the nonlinear load and to make the supply currents sinusoidal. To fulfill these demands, the traditional control scheme requires a harmonic detector and current controller where both loops must be designed properly to achieve good control performance. However, it may cause excessive complexity in the design process.

B. Proposed Control Strategy

In order to simplify the control scheme and to enhance the accuracy of the APF, an advanced control strategy is proposed, as shown in Fig. 2. In Fig. 2, the proposed control scheme is implemented by using only the supply current (i_{Sa} and i_{Sb}) without detecting the load current ($i_{L,abc}$) and filter current ($i_{F,abc}$). Thereby, the load current sensors and filter current sensors in the typical shunt APF shown in Fig. 1 can be eliminated. And also, the harmonic current detection is omitted. Due to the absence of harmonic detection, the proposed control scheme can be implemented with only two loops: the outer voltage control and the inner current control. The outer loop aims to keep dc-link voltage of the APF constant through a PI controller, which helps the APF deal with load variations. The output of this control loop is the reference active current in the fundamental reference frame (i^*_{Sd}). Meanwhile, the reference reactive current (i^*_{Sq}) is simply set to be zero, which ensures the reactive power provided by the power supply to be zero. And, the reactive power caused by loads is supplied by the shunt APF. The inner loop is then used to regulate the supply current in the fundamental reference frame ($i_{S,dq}$) by using the proposed ANN current controller. The output of this loop becomes the control signal ($v_{F,ab}$ *) applied to the four-switch APF which is implemented by the FSTPI. Since the current control is executed without the harmonic detector, the control performance of the APF only relies on the current controller. In the next section, the analysis and design of the proposed current controller will be presented.

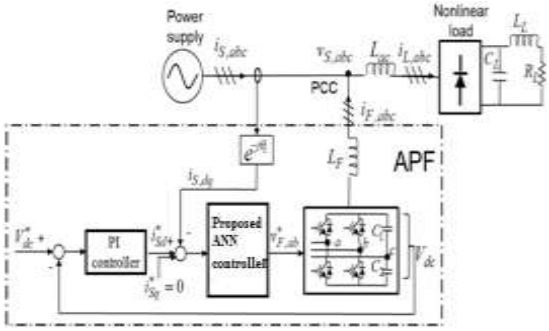

Fig.2. Structure of the proposed control scheme for three-phase shunt APF

III. DESCRIPTION OF THE WHOLE CONTROL STRATEGY

Fig.3 illustrates the block diagram of whole proposed control strategy. As aforementioned, the proposed control scheme contains two main loops: the dc-link voltage control and the supply current control. In addition, since the proposed current controller is employed in the fundamental reference frame, a phase-locked loop (PLL) is required to track the phase of the supply voltage which is needed for coordinate transformation and synchronization.

A. DC-Link Voltage Control Loop

As stated earlier, this control loop aims to keep dc-link voltage of the shunt APF constant through a simple PI regulator, whose output is the reference active current in the fundamental reference frame as Follows

$$I_{sd}^* = (K_{pdc} + (K_{idc}/S))(V_{dc}^* - V_{dc}) \quad (1)$$

where K_{pdc} and K_{idc} are the proportional and integrator gains of the PI controller, respectively, and V_{dc*} and V_{dc} are reference and measured dc-link voltages of the APF, respectively. In fact, since the four-switch APF has only two switching legs, the four-switch APF needs a higher dc-link voltage reference (V_{dc*}) compared to the traditional six-switch APF as mentioned in Table I. In addition, since the dc-link voltage of the APF contains small ripples at harmonic frequencies due to harmonic currents, a low-pass filter (LPF) is designed to eliminate all ripples in the feedback measurement of the dc-link voltage, which helps in smoothing the reference current i^*_{Sd}.

In the proposed control scheme, the role of the dc-link voltage controller is not only to ensure a proper operation of the APF but also to help the APF deal with load variations. In this paper, even though the load current measurement is not used, the load changes can be detected indirectly through dc-link voltage variations. Hence, by detecting and regulating the dc-link voltage, the shunt APF can recognize and respond against load variations without the load current measurement.

B. Supply Current Control Loop

This loop regulates the supply current by means of the proposed current control scheme shown in Fig. 6.

The reference active current i^*_{Sd} is the output of the dc-link voltage control loop given in (13), while the reference reactive current i^*_{Sq} is simply set to be zero. Consequently, the reactive power caused by loads can be fully compensated by the APF, and also unity power factor condition is achieved at the supply side.

C. Control Signal Computation for the Four-Switch APF

The traditional three-phase VSI is commonly used to implement an APF. In this paper, in order to accomplish a low-cost APF topology, the four-switch APF is introduced by replacing the traditional three-phase VSI with the FSTPI without degrading the performance of the proposed control strategy. The FSTPI, which is composed of four power switching devices and two split capacitors, has been applied for low-cost ac motor drives [27], [28]. In Fig. 9, the control signal in the stationary reference frame ($v_{F,\alpha\beta*}$) obtained after executing the current controller is changed into control signals of the four-switch APF as the following equations:

$$v_{Fa*}=\sqrt{(3/2)}\ v_{F\alpha*}+*\sqrt{(1/2)}\ v_{F\beta*}v_{Fb*}=\sqrt{(2)}\ v_{F\beta*} \qquad (2)$$

where v_{F*a} and v_{F*b} are the control signals for leg a and b of the four-switch APF, respectively.

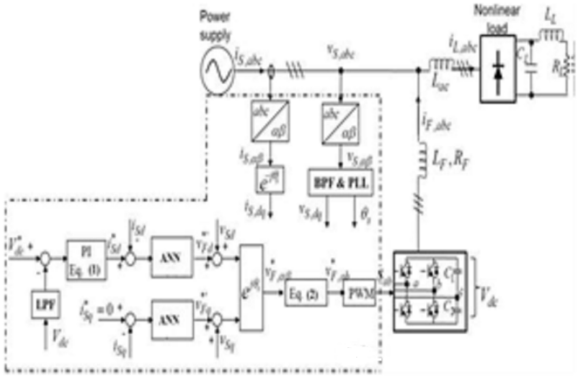

Fig.3. Block diagram of proposed control scheme

D. Supply Voltage PLL

The aim of this loop is to track the phase of the supply voltage, which is a necessary component for any converter interfacing with grid. In practical distribution network, supply voltage is regularly not pure sinusoidal but contains harmonic components, which may affect to the accuracy of the PLL. To overcome this problem, a band pass filter (BPF) tuned at the fundamental frequency of the supply voltage is implemented to reject all of the harmonic components contained in supply volt-age, and its output contains only the fundamental component which is used as the input of the PLL block. The block diagram of the improved PLL is illustrated in Fig. 4. Even though the BPF used in the PLL can cause a small time delay in tracking the phase angle of the supply voltage, it is negligible because the PLL usually operates at steady state condition before the APF is active.

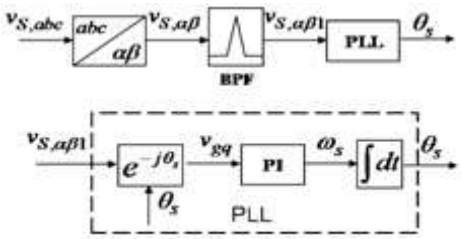

Fig.4. Block diagram of the improved PLL

IV. DESIGN OF ANN CONTROLLER

A. Artificial Intelligence Tools

Artificial intelligence is a fast growing discipline that attempts to represent and manipulate knowledge to automatically solve problems that before were only solved by humans (Rich and Knight, 1991). Because of the complex nature of the project recommendation, prioritization and selection processes in a PMS, artificial intelligence techniques are useful tools that can be applied to these processes. Two artificial intelligence techniques, expert systems and artificial neural networks, were found particularly appealing for the screening and selection of candidate roadway sections. Each has advantages and disadvantages. Neural networks have the ability to make associations between known inputs and outputs by observing a large number of examples. They do not require the development of knowledge rules, are capable of learning from examples, have greater generalization capabilities, are able to produce correct or near correct responses when presented with partially incorrect or incomplete data, are faster to develop and allow easier updating of the knowledge base. On the other hand, expert systems require the development of rules for the knowledge-base and provide better explanation capabilities. The neural network approach was preferred because:

1) The selection process is relatively unstructured, making the development of rules particularly complicated

2) Considers uncertain and sometimes incomplete data, and

3) The degree of detail of the available information varies from section to section in the database. Artificial neural networks mimic the human brain.

The human brain is complex network of hundreds of millions of neurons that send information back and forth to each other though connections. The result is an intelligent being able of learning, analysis, prediction, and recognition. Artificial neural networks are composed by many simulated neurons or units that are connected in such a way that are able to learn in a similar manner to people (Lawrence, 1994). The most important characteristics of neural networks are that they are able to produce correct or near correct responses when presented with partially incorrect or incomplete data, and they are able to generalize rules from the cases on which they are trained and apply them to new inputs. There are several ways the network can "learn." The most common learning method, used by the network developed, is by example and repetition, also called back propagation (Lawrence, 1994). Many example pairs of inputs and outputs are presented to the network, which adjusts the weights of the connections to minimize the number of wrong predictions.

The examples that are presented to the network are called the training set. The learning or training is an iterative process. Each time it is presented with an input (the condition of a particular roadway section), the network "guesses" what the output is supposed to be. If the network output differs from the one presented (a section that was not programmed is recommended), the weights of the connections are adjusted. Each training case, with the corresponding modifications of connections, is called a cycle. A set of cycles, made up of one cycle for each training case, is called an epoch. The weights are modified many times until the network gets an acceptable number of right answers or the number of epochs exceeded a prescribed maximum. It is common that an artificial neural network requires thousands of epochs to learn most of the examples.

B. Design Of The Artificial Neural Network

The design of the artificial neural network included the following steps:

1) Selection of an artificial neural network scheme.
2) Data preparation and selection of input and output parameters.
3) Selection of the most appropriate network architecture and training Parameters.
4) Refinement of the artificial neural network.

B. Artificial Neural Network Scheme

Several types of artificial neural network types were considered, and the use of a commercial software package was weighted against the possibility of developing a specific neural network simulator. Based on the literature reviewed, a back propagation neural network appeared to be the most appropriate type for this type of application. Fortunately several good simulation software packages were available for this type of networks. After reviewing the various options, the commercial software package Brain Maker was selected. It is a back propagation simulator that works in both DOS and WINDOWS environments, and has very good utilities for data preparation and manipulation (CSS, 1993). Figure 1 shows the scheme of the three-layer back propagation neural network simulator adopted. An input processor program interfaces with the PMS database; it uses the average section characteristics computed by the delineation procedure and stratifies some of the data fields. The outputs of the input processor are a set of values *Ii* used to activate the artificial neurons in the input layer of the artificial neural network simulator. An *Ii* is computed for each parameter included in the decision process (roughness, cracking, ADT, etc.).

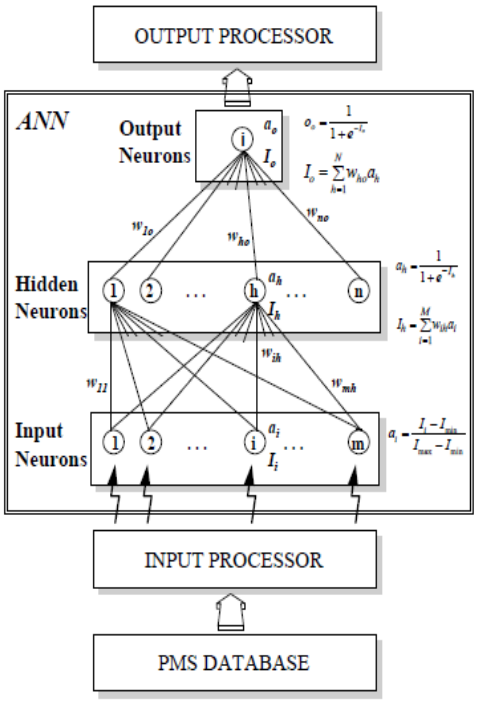

Fig5. Scheme of the Artificial Neural Network Developed

The artificial neural network simulator processes the *Ii*'s corresponding to each section and determines if the section should be recommended or not. It is organized in three layers of neurons, the *input neurons*, that receive the information from the input processor, the *hidden neurons* that link the neurons in the other two layers, and the *output neurons* (only one in this case) that sends the results to the output processor. The first step conducted by the neural network simulator is to process the input of each neuron *i* of the input layer, *Ii*, to a scale of 0 to 1; this is the activation level, *ai*, of the neuron *i.* The scaled values or activation levels are transmitted to all connected neurons in the hidden layer. At the hidden layer, each neuron *h* computes its input, *Ih*, adding the level of activation (*ai*) of all connected input neurons weighted by the weights of the connections (*wih*). This input *Ih* is then processed to an activation level, *ah*, using an *activation function, ah* = f*(Ih)*. At the output layer, the input for the output neuron, *Io*, is computed adding the *ah* 's of the connected hidden neurons weighted by the connection weights (*who*). This input *Io* is processed to the output of the network using the activation formula. Finally, the output processor translates the numeric output received from the simulator to a recommendation. In the training examples, a section that was programmed was assigned an output of 1, and one that was not

programmed an output of 0. Since the output of the network is not necessarily a 0 or 1, but a number between these two limits, a breakdown value of 0.5 was adopted to differentiate between a section that should be recommended and one that should not.

V. SIMULATION RESULTS

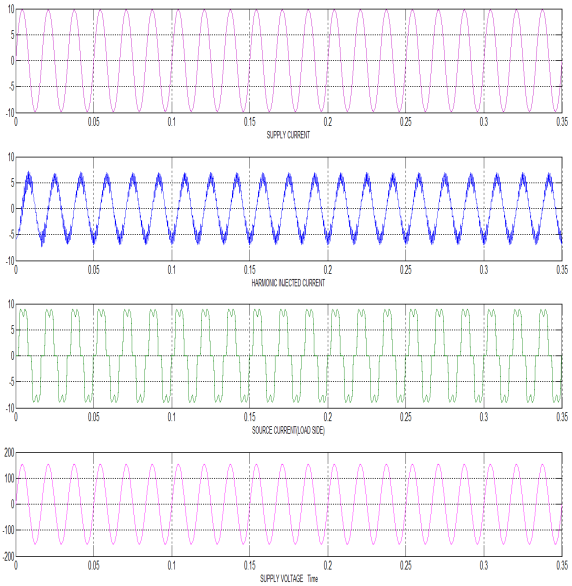

Fig.7. Steady-state performance with proposed Ann control scheme under RL load

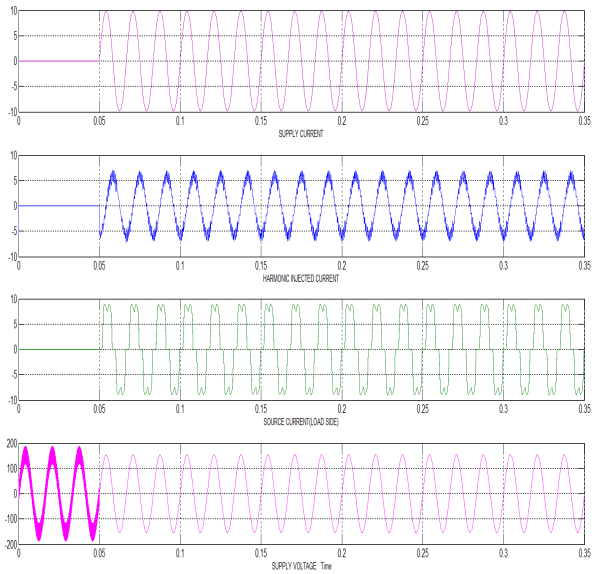

Fig.8.1 Dynamic response of proposed Ann control scheme under RL load applied

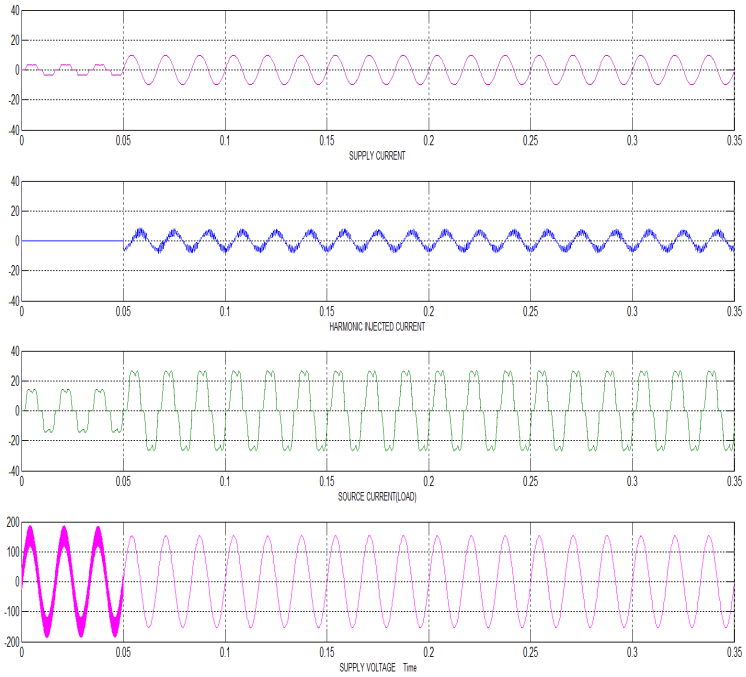

Fig.8.2Dynamic response of proposed control scheme under RL load changed.

As that shown in Fig. 7, it was carried out by using the proposed Ann control scheme. The results are presented in Fig.7. Fig.7shows that the harmonic currents are effectively compensated and the supply current is almost sinusoidal with a small THD factor of approximately 2.3% whereas the load current is highly distorted with the THD factor of 25.2%. From these results, the effectiveness of the proposed Ann control scheme is verified: harmonic currents are effectively compensated without load current measurement

and harmonic detector. In addition, the proposed Ann control scheme avoids the presence of notches in the supply current caused by the inaccurate harmonic tracking performance of the harmonic detector as reported in [13], [24]. To evaluate the dynamic performance of the proposed control strategy with load variations, the transient responses of the APF with the load applied or changed are shown in Fig.8.1and 8.2, respectively.

As shown in Fig. 8, as soon as the load is applied or changed, the filter current quickly responds to changes to compensate harmonic currents in the load and to ensure that the supply current sinusoidal and in-phase with the corresponding supply voltage. In fact, due to the effect of the LPF in the dc-link control loop, the response time of the supply current is minimally increased, but it is not longer than one period of the supply voltage. Likewise, the proposed Ann control strategy is also performed with a nonlinear RLC load, where the steady-state performance and dynamic response are shown in Figs. 9 and 10 respectively. In Fig. 9, the supply current is very close to sinusoidal with a low THD factor of approximately 2.24% while the THD of load current is very high, about 32.2%. In Fig. 10, the filter current also quickly responds to the load variations to compensate the harmonic currents in the supply. The supply current becomes close to sinusoidal with its response time of less than one period of the supply voltage. It is verified through experiments that the proposed control strategy has good steady-state performances as well as good dynamic responses with both nonlinear RL and RLC loads. In majority of previous studies, the supply voltage has usually been assumed to be an ideal sinusoidal, but this voltage condition is rare in practical networks. The non-sinusoidal supply voltage condition in practical networks may adversely affect the control performance of the APF. To verify the effectiveness of the proposed control algorithm under such conditions, experiments were carried out where the supply voltage was injected with fifth and seventh harmonic components of 10% and 5% magnitudes of the fundamental component, respectively. The results are illustrated in Fig. 11. As shown in Fig. 11, the harmonic compensation performance of the APF is not deteriorated by the distorted supply condition where the supply current was also close to sinusoidal and similar with the results shown in Figs. 8 and 10 where an ideal sinusoidal supply voltage is given. There are only small increases in THD factors, approximately 2.24% and 2.28% for the cases of nonlinear RL and RLC loads, respectively.

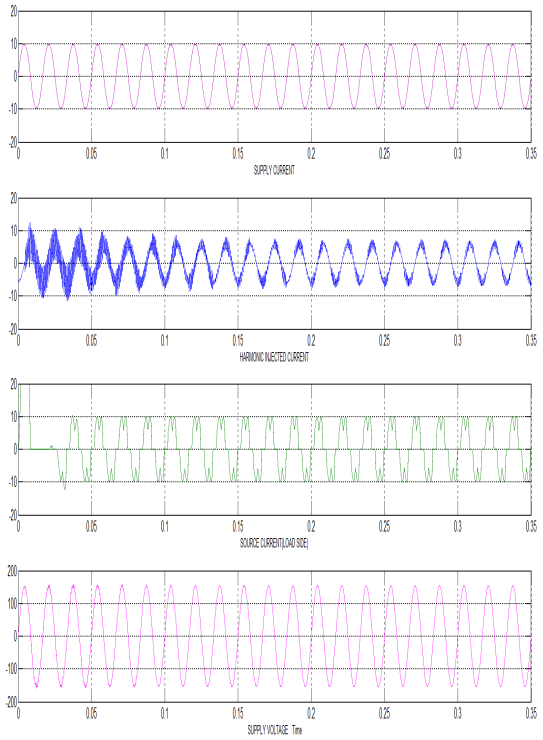

Fig.9. Steady state performance with proposed Ann control scheme and RLC Load.

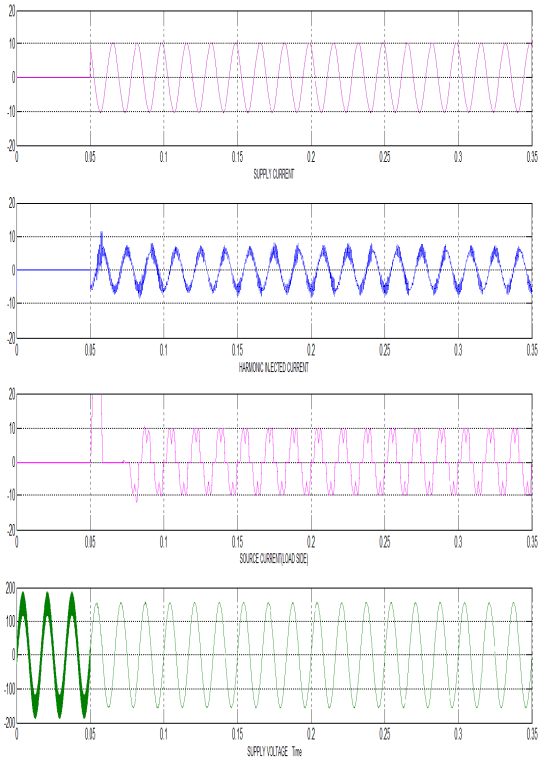

Fig.10. Dynamic response of proposed Ann control scheme under RLC load applied.

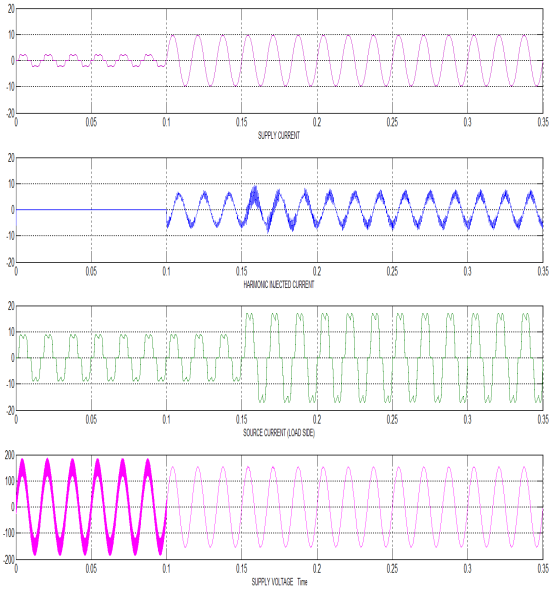

Fig.10. Dynamic response of proposed Ann control scheme under RLC load changed.

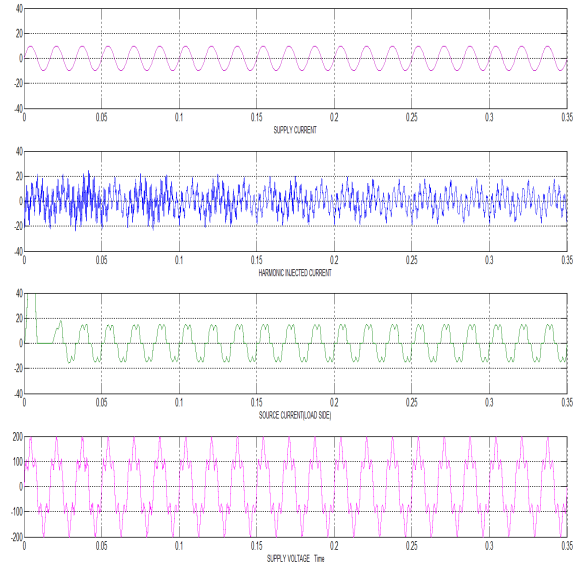

Fig.11. Steady state performance of the proposed Ann control scheme under distorted supply voltage condition with RL load.

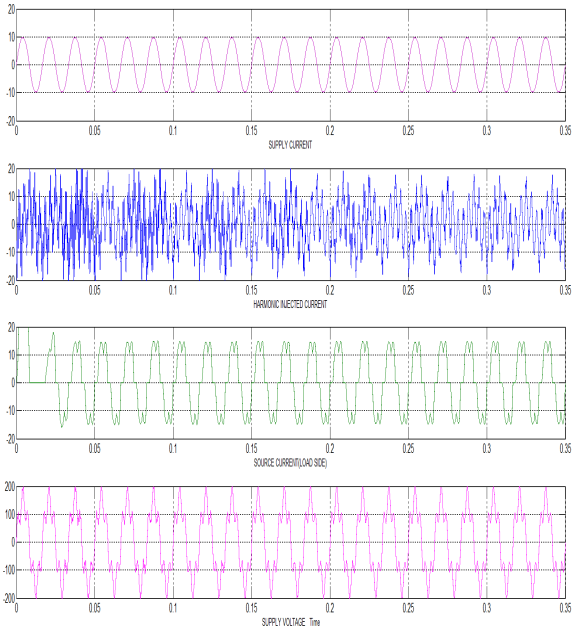

Fig.11. Steady state performance of the proposed Ann control scheme under distorted supply voltage condition with RLC **load.**

The results demonstrate that the proposed Ann current controller achieves good performances under ideal sinusoidal as well as distorted supply conditions. The THD of the supply current is reduced to less than 2.3% for all cases. In contrast, such good performances cannot be achieved by using the traditional PI current controller. In the previous APFs, the THD values of the compensated supply current are normally around 2–5%, and the lowest THD up to now is about 1.2% in [18]. Even though the THD of the proposed Ann current controller cannot reach the lowest value in [18], its THD is sufficiently small as compared with the results achieved in the other papers. Furthermore, the proposed APF is much cheaper since it uses only two current sensors and four switching devices. As a result, we can say the proposed APF has very good performance in spite of the reduced hardware, and it can be considered as a low-cost high-performance APF.

VI. CONCLUSION

In this paper, an advanced control strategy with ANN for the three-phase shunt APF was proposed. The proposed control strategy presents good steady-state performance with nonlinear RL and RLC loads as well as good dynamic response against load variations. The supply current is almost perfect sinusoidal and in-phase with the supply voltage even under the distorted voltage condition. Moreover, we also confirmed that the FSTPI can be used to implement the APF without any degradation in the APF performance. Elimination of harmonic detector and usage of four switch three phase inverter is used to reduce the overall cost of the system.ANN technique is used to further reduce the THD of supply current, dynamic response also improved with proposed ANN current controller. THD factor of the supply current was reduced to less than 2.3%.

REFERENCES

[1] *Recommended Practice for Harmonic Control in Electric Power Systems*, IEEE Std. 519-1992, 1992.
[2] *Limits for Harmonic Current Emission*, IEC 61000-3-2, 2001.
[3] H. Akagi, ―New trends in active filters for power conditioning, *IEEE Trans. Ind. Appl.*, vol. 32, no. 2, pp. 1312–1332, Nov./Dec. 1996.
[4] F. Z. Peng, ―Application issues of active power filters, *IEEE Ind. Appl. Mag.*, vol. 4, no. 5, pp. 21–30, Sep./Oct. 1998.
[5] H. Akagi, E. H. Watanabe, and M. Aredes, *Instantaneous Power The-ory and Applications to Power Conditioning*, M. E. El-Hawari, Ed. New York: Wiley, 2007.
[6] S. Buso, L. Malesani, and P. Mattavelli, ―Comparison of current control techniques for active filters applications,‖ *IEEE Trans. Ind. Electron.*, vol. 45, no. 5, pp. 722–729, Oct. 1998.
[7] L. Malesani, P. Mattavelli, and S. Buso, ―Robust dead-beat current control for PWM rectifiers and active filters, *IEEE Trans. Ind. Appl.*, vol. 35, no. 3, pp. 613–620, May/Jun. 1999.
[8] S. Rahmani, N. Mendalek, and K. Al-Haddad, Experimental design of a nonlinear control technique for three-phase shunt active power filter,‖ *IEEE Trans. Ind. Electron.*, vol. 57, no. 10, pp. 3364–3375, Oct. 2010.
[9] H. Hu, W. Shi, Y. Lu, and Y. Xing, ―Design considerations for DSP-controlled 400 Hz shunt active power filter in an aircraft power system,‖ *IEEE Trans. Ind. Electron.*, vol. 59, no. 9, pp. 3624–3634, Sep. 2012.
[10] Z. Chen, Y. Luo, and M. Chen, ―Control and performance of a cascaded shunt active power filter for aircraft electric power system,‖ *IEEE Trans. Ind. Electron.*, vol. 59, no. 9, pp. 3614– 3623, Sep. 2012.
[11] L. Asiminoaei, F. Blaabjerg, and S. Hansen, ―Detection is key—Harmonic detection methods for active power filter applications,‖ *IEEE Ind. Appl. Mag.*, vol. 13, no. 4, pp. 22–33, Jul.Aug.2007.
[12] R. R. Pereira, C. H. da Silva, L. E. B. da Silva, G.Lambert-Torres, and J. O. P. Pinto, ―New strategies for application of adaptive filters in active power filters,‖ *IEEE Trans. Ind. Appl.*, vol.47, no. 3, pp. 1136–1141, May/Jun. 2011.
[13] Bhattacharya and C. Chakraborty, ―A shunt active power filter with en-hanced performance using ANN-based predictive and adaptive control-lers,‖ *IEEE Trans. Ind. Electron.*, vol. 58, no. 2, pp. 421–428, Feb. 2011.
[14] F. A. S. Neves, H. E. P. de Souza, M. C. Cavalcanti, F. Bradaschia, and E. J. Bueno, ―Digital filters for fast harmonic sequence component separation of unbalanced and distorted three-phase signals,‖ *IEEE Trans. Ind. Electron.*, vol. 59, no. 10, pp. 3847–3859, Oct. 2012.
[15] R. I. Bojoi, G. Griva, V. Bostan, M. Guerriero, F. Farina, and F. Profumo, ―Current control strategy
for power conditioners using sinusoidal sig-nal integrators in synchronous reference frame,‖ *IEEE Trans. Power Electron.*, vol. 20, no. 6, pp. 1402–1412, Nov. 2005.
[16] C. Lascu, L. Asiminoaei, I. Boldea, and F. Blaabjerg, ―Frequency response analysis of current controllers for selective harmonic
[17] compensation in active power filters,‖ *IEEE Trans. Ind. Electron.*, vol. 56, no. 2, pp. 337– 347, Feb. 2009.
[18] L. Limongi, R. Bojoi, G. Griva, and A. Tenconi,―Digital current-control schemes,‖ *IEEE Ind. Electron. Mag.*, vol. 3, no. 1, pp. 20–31, Mar. 2009.
[19] C. Lascu, L. Asiminoaei, I. Boldea, and F. Blaabjerg, ―High performance current controller for selective harmonic compensation in active power filters,‖ *IEEE Trans. Power Electron.*, vol. 22, no. 5, pp. 1826–1835, Sep. 2007.
[19] B. N. Singh, A. Chandra, and K. Al-Haddad, ―Performance comparison of two current control techniques applied to an active filter,‖ in *Proc. 8th ICHQP*, Athens, Greece, Oct. 14–16, 1998, vol. 1, pp. 133–138.
[20] J. W. Dixon, J. M. Contardo, and L. A. Moran, ―A fuzzy-controlled active front-end rectifier with
current harmonic filtering characteristics and minimum sensing variables,‖ *IEEE Trans. Power Electron.*, vol. 14, no. 4, pp. 724–729, Jul. 1999.
[21] M. Singh, V. Khadkikar, and A. Chandra, ―Grid synchronization with harmonics and reactive power compensation capability of a permanent magnet synchronous generator-based variable speed wind energy conver-sion system,‖ *IET Power Electron.*, vol. 4, no. 1, pp. 122–130, Jan. 2011.
[22] A. Szromba, ―Energy controlled shunt active power filters,‖ *Int. J. Com-put. Math. Elect. Electron. Eng.*, vol. 26, no. 4, pp. 1142–1160, Jan. 2007.
[23] E. Teresa and J. A. Pomilio, ―Shunt active power filter synthesizing re-sistive load,‖ *IEEE Trans. Power Electron.*, vol. 17, no. 2, pp. 273–278, Mar. 2002.
[24] B. N. Singh, B. Singh, A. Chandra, P. Rastgoufard, and K. Al-Haddad, ―An improved control algorithm for active filters,‖ *IEEE Trans. Power Del.*, vol. 22, no. 2, pp. 1009–1020, Apr. 2007.
[25] F. Blaabjerg, D. Neacsu, and J. K. Pedersen, ―Adaptive SVM to compen-sate DC-Link voltage ripple for four-switch three-phase,‖ *IEEE Trans. Power Electron.*, vol. 14, no. 4, pp. 743–752, Jul. 1999.
[26] M. B. de R. Corrêa, C. B. Jacobina, E. R. C. da Silva, and A. M. N. Lima, ―A general PWM strategy for four-switch three phase inverter,‖ *IEEE Trans. Power Electron.*, vol. 21, no. 6, pp. 1618–1627, Nov. 2006.

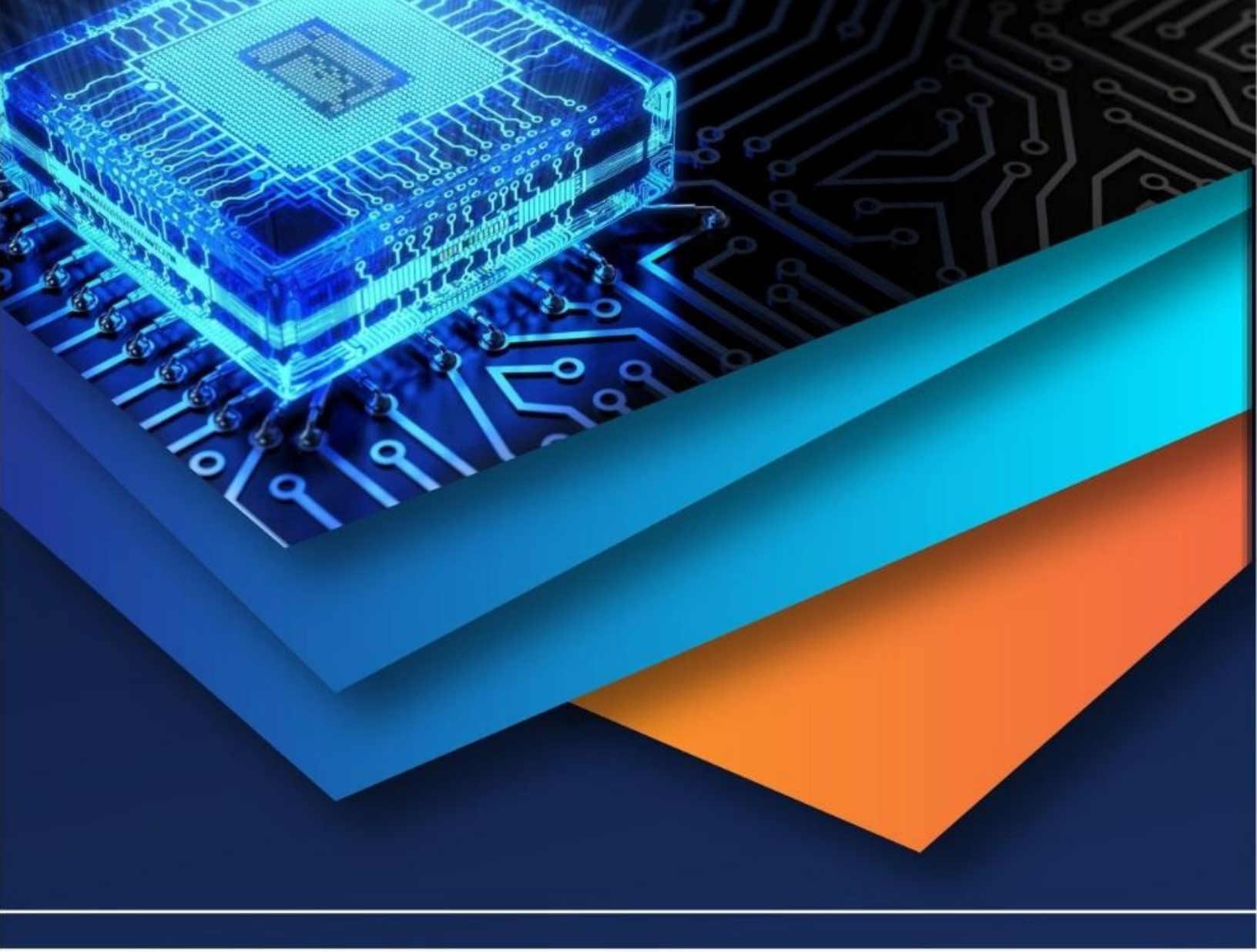

10.22214/IJRASET

45.98

IMPACT FACTOR: 7.129

IMPACT FACTOR: 7.429

INTERNATIONAL JOURNAL FOR RESEARCH

IN APPLIED SCIENCE & ENGINEERING TECHNOLOGY